
Assessment of a Next Generation Gravity Mission (NGGM) for monitoring the Variation of the Earth's Gravity Field

ESA Contract 22643/09/NL/AF

TN3_IAPG: From Science to Sensor requirements
TN3: Observing Techniques and Instrument Concepts

Doc. No.: NGGM_SCI_TN3_IAPG
Issue: 1 Draft
Revision: 0
Date: 30-July, 2010

Author:

Michael Murböck
IAPG, Institut für Astronomische und Physikalische Geodäsie, TU München
murboeck@bv.tum.de

Table of Contents

| | | |
|-------|--|----|
| 1 | Abstract | 3 |
| 2 | Prioritization..... | 3 |
| 3 | Nominal Mission Profile Requirements | 4 |
| 4 | Simulations..... | 5 |
| 4.1 | Ranging System..... | 5 |
| 4.1.1 | White noise PSD | 5 |
| 4.1.2 | Coloured noise PSD | 6 |
| 4.1.3 | Simulation results..... | 7 |
| 4.2 | Accelerometer | 9 |
| 4.3 | Alternative error scenario | 11 |
| 4.4 | GNSS..... | 14 |
| 4.5 | Gradiometry | 15 |
| 4.5.1 | Sensitivity..... | 15 |
| 4.5.2 | Redundancy and CGE | 16 |
| 5. | Summary | 18 |
| 5.1 | Alternative error scenario | 20 |
| 6. | Appendix | 21 |
| | Appendix A: Error propagation for linear trend estimation..... | 21 |
| | Appendix B: Simulation results | 22 |
| 7. | References | 28 |

1 Abstract

This document is submitted with the intent of clarifying the science requirements for a NGGM. The first step is the synthesis of information, which are defined in two documents according to WP1100, which have been submitted to ESA as part of this study. These documents are the WP1100 Report and the WP1100 Requirements Analysis Progress Report (see References 1. and 2.).

The first step is the clarification of prioritizations in terms of spatial and temporal coverage and the scales of the signals, which should be observed by the NGGM. A more difficult but necessary task will be the description of the magnitudes of these signals in terms of geoid heights, gravity potential and equivalent water layer thickness (EWLT). It is clear, that these values depend on the spatial and temporal resolution as defined by the mission but also on the location. These magnitudes directly produce a maximum tolerance for the cumulative errors of a NGGM gravity field solution. Thus, with several simulations one can define observation requirements. The requirements represent a description of noise power spectral densities (PSDs) of the distance measurements in terms of range rate or range acceleration and of accelerometer noise. The contributions of GNSS and gradiometer observations to such a mission are discussed in a further section.

It is clear, that there are several other error sources, which will also affect the gravity field solution. The point of this document however, is to evaluate only the signal magnitudes, signal resolutions and the resulting sensor noise structure.

2 Prioritization

Chapter 8 of the WP1100 Report describes four fields of primary focus for an NGGM. These are ice, continental water, ocean masses and solid-earth. The Table in Chapter 8.6 of the document provides a rated list of different signals. The four highest rated signals are listed below in Table 1. Their different attributes, i.e. signal magnitude at a particular temporal scale, are taken from the documents referred to above. The table lists only the signals of interest to the NGGM. The numbers presented in the table, represent approximate magnitudes, which we use to derive the observation requirements. The numbers in the table are only given in terms of geoid heights. Using the following rule of thumb one can easily derive EWLT or gravity potential (only the order of magnitudes is relevant). Of course the conversion to EWLT from the other two units is frequency dependent. The higher the frequency or the higher the spherical harmonic (SH) degree the less accurate is this rule of thumb.

$$1 \left[\frac{m^2}{s^2} \right] GravityPotential \approx 0.1 [m] GeoidHeight \approx 1 [m] EWLT$$

| | <i>Description</i> | <i>Spatial resolution</i> | <i>Temporal resolution</i> | <i>Signal magnitude in geoid heights</i> |
|---|---|---------------------------|-----------------------------|--|
| 1 | Melting of ice sheets (with separation of GIA) | 100 – 1000 km | Seasonal – secular | 0.01 mm/year (secular) |
| 2 | Non-steric comp. of sea-level var. at seasonal and shorter time scales | Global to basin level | Interannual – secular | 0.1 mm/year (secular) |
| 3 | Ground water (soil moisture and snow) at larger spatial scales | 10 – 200 km | Hourly – seasonal – secular | 1 cm (seasonal) |
| 4 | Post-seismic deformation | 10 – 200 km | Subseasonal | 1 mm (subseasonal) |

Table 1: Fields of Prioritization with their spatial and temporal resolution and approximate signal magnitudes (see References 1. and 2.)

3 Nominal Mission Profile Requirements

Before defining observation requirements one must define a nominal mission profile. The scientific requirements demonstrate that it is not very important to reach a temporal resolution shorter than 1 month. Of course a NGGM with improvements in monthly data with a subcycle of a few days will also provide interesting information for these time scales. Another benefit would be reduction of temporal aliasing.

The nominal repeat cycle will be 30 days and the nominal mission life time 11 years (long term trends, solar cycle). And because of societal and scientific priorities for observing the Polar Regions (ice masses) an inclination of close to 90 degrees will be part of the nominal profile.

The next step is the translation of the numbers in Table 1 into maximum cumulative geoid errors (CGE) for the nominal mission. Therefore the desired secular signal magnitudes of ice mass variations (1) and sea-level variations (2) are translated into monthly values. For that purpose, values ten times larger for the monthly measurements (0.1 mm for 1 and 1 mm for 2) is sufficient (See Appendix A).

A wavelength λ in km can be approximately transformed into SH degree L with

$$L = \frac{20000km}{\lambda}.$$

With these assumptions one can derive the following Table 2 of requirements for the monthly gravity field in terms of maximum CGE.

| | | Wavelength | 10000 km | 1000 km | 200 km | 100 km | 10 km | |
|-----|--------|------------|----------|---------|--------|--------|-------|--|
| | | SH degree | 2 | 20 | 100 | 200 | 2000 | |
| CGE | 10 mm | | | | 3 | | | |
| | 1 mm | 2 | | | | 4 | | |
| | 0.1 mm | 1 | | | | | | |

Table 2: Requirements in terms of max. CGE for monthly solutions (The numbers in the grey boxes correspond to the first column of Table 1)

The next step is a restriction of the values in Table 2 to more realistic requirements for the CGE of the gravity field solution of a NGGM. Therefore the three boxes (3, 4 and 1) will be reduced to smaller SH degrees (shaded areas). In any case, a compromise is required to get to the values in Table 3. On a monthly basis it makes no sense to require a 0.1 mm geoid up to SH degree 200 or a 1 cm geoid up to SH degree 2000. In this case, a first step of iteration could be the following values for CGEs. The NGGM should provide gravity information up to SH degree 250 and the cumulative geoid error for the SH degrees 150, 200 and 250 should be not greater than 0.1, 1 and 10 mm respectively. From this point of view the signals in Table 1 will be observable to a large extent in spatial resolution and with a temporal resolution of one month.

| | | | |
|-----------|-----|-----|-----|
| SH degree | 150 | 200 | 250 |
| CGE [mm] | 0.1 | 1 | 10 |

Table 3: Requirements for CGE

4 Simulations

From these requirements, semi-analytical simulations for different sensor systems can be performed to investigate, how much of the requirements can be fulfilled with which noise PSD. By propagating observation noise in terms of noise PSDs, these simulations estimate variance-covariance matrices of SH coefficients. As this exercise represents only error propagation, it is clear that this approach cannot take aliasing and other analysis technique problems into account. In the following chapters, simulation results can be seen in terms of CGE. These are global mean values. For any mission, the error distribution will mainly depend on the latitude. For polar missions, the lowest errors will be at the poles. For non-polar orbits, the errors will increase dramatically for latitudes without observations. The figures we present contain results of simulations for nominal distances between the satellites, $d \in \{50, 100, 200, 300\}$ km, and different mission altitudes $h \in \{300, 350, 400, \dots, 550\}$ km. The simulations are computed up to SH degree and order 250. For every simulation, three numbers are provided according to the three error levels (0.1, 1 and 10 mm). These are the SH degrees, up to which the simulated mission stays under each of the three error levels. Later, these values should be used as an indicator for the definition of the sensor requirements.

4.1 Ranging System

4.1.1 White noise PSD

Range rate observations are taken as measurements. White noise is assumed for the noise of the range rate observations. In terms of range rate, this represents a noise increasing with the frequency (see dashed lines in Figure 1). The PSD can be written as $PSD = a \cdot d$ in

$\left[\frac{m}{\sqrt{\text{Hz}}} \right]$ (a in $\text{Hz}^{-0.5}$ and d in m), where d is the distance between the two satellites and a is chosen from $\{n \cdot 10^{-14}, n \cdot 10^{-13}, n \cdot 10^{-12}\}$ with $n \in \{1, 2, \dots, 10\}$.

4.1.2 Coloured noise PSD

Again range rate observations are taken as measurements. A typical noise PSD for such an observation looks like the solid lines in Figure 1 and can be computed from

$$PSD = d \cdot \begin{cases} a \cdot 10^{-2} \cdot f^{-1} & \text{for } f < 10\text{mHz} \\ a & \text{for } f \geq 10\text{mHz} \end{cases} \text{ in } \left[\frac{m}{\sqrt{\text{Hz}}} \right],$$

where d is distance and a is the

white noise level for high frequencies. The values used for a are the same as for the white noise case. The image on the left of Figure 1 shows the PSDs in terms of range observations as described in the formula. The image on the right shows the PSD in terms of range rate observations (Multiplication with $2\pi f$). The definitions of these PSD functions can also be found in the document presented by ThalesAlenia at the first Progress Meeting in Turin (See References 3.).

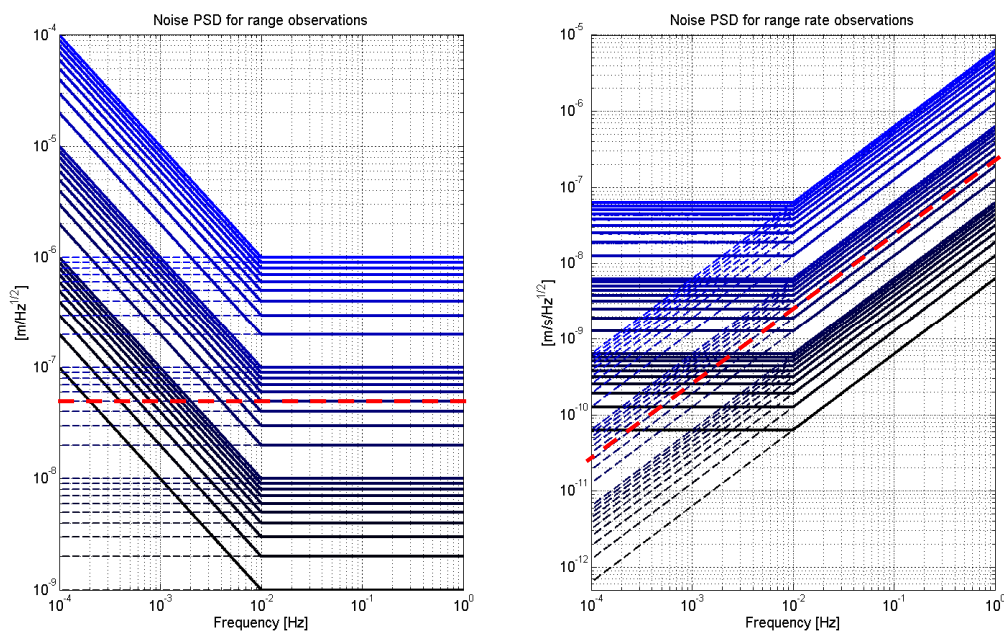


Figure 1: Noise PSD in terms of range and range rate observations for the SST sensor system for the distance between the satellites of 100 km (solid lines: coloured noise, dashed lines: white noise, red lines: Previous NGGM study limit)

4.1.3 Simulation results

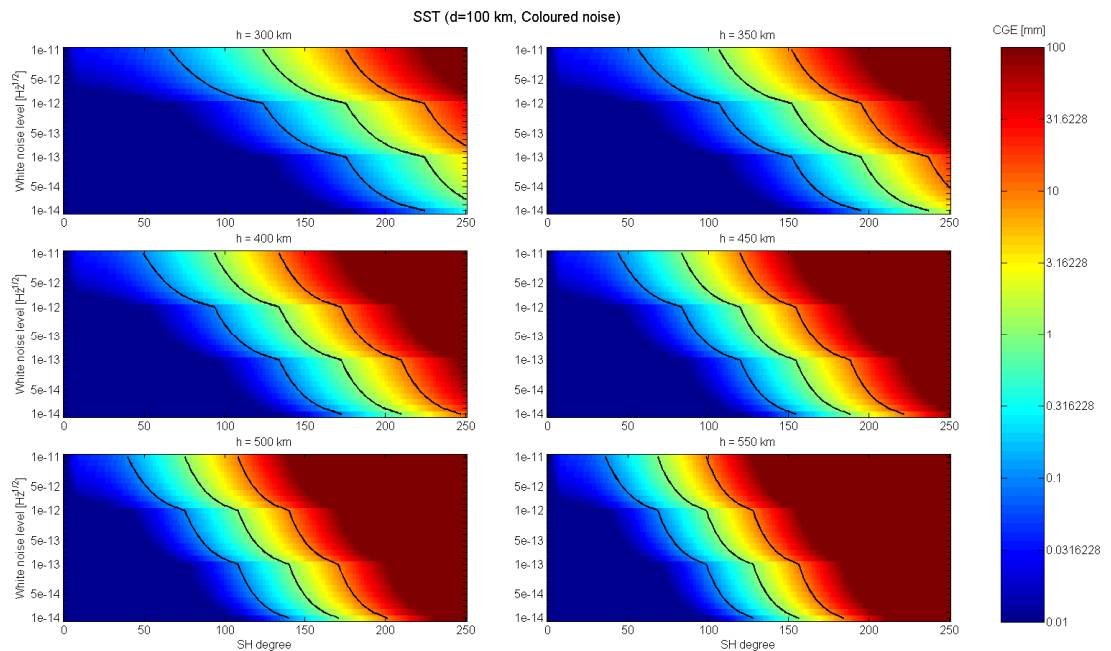


Figure 2: Cumulative Geoid Error for the SST sensor system for $d=100$ km, coloured noise case (the three black lines in each plot represent the CGE levels 0.1, 1 and 10 mm)

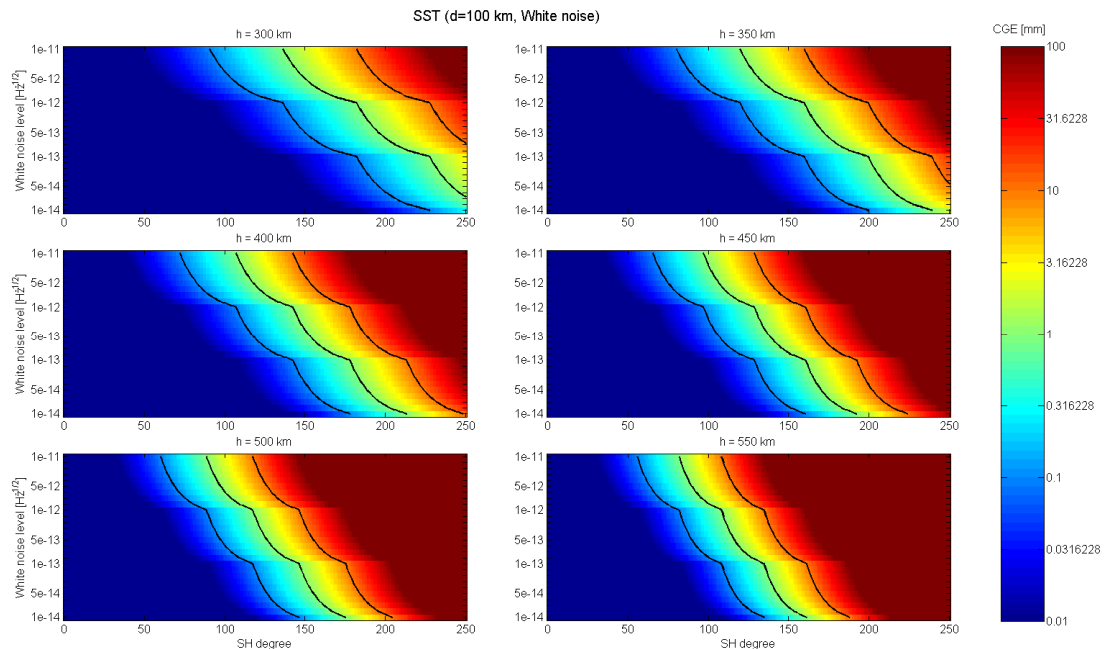


Figure 3: Cumulative Geoid Error for the SST sensor system for $d=100$ km, white noise case (the three black lines in each plot represent the CGE levels 0.1, 1 and 10 mm)

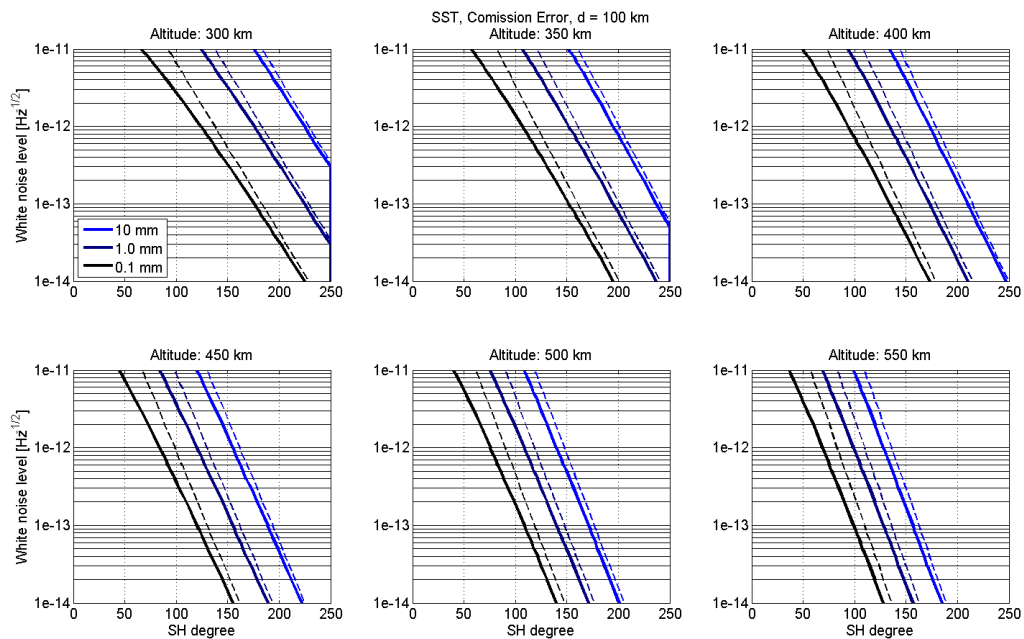


Figure 4: Requirement lines for the SST sensor for $d=100$ km (solid lines: coloured noise, dashed lines: white noise)

The results of the simulations for $d=100$ km can be seen in the Figures 2, 3 and 4. The results for the other distances are figured in Appendix B. In Figure 2 (coloured noise case) and 3 (white noise case), CGEs for the six different altitudes and the 28 different white noise levels can be observed. Figure 4 shows the SH degrees, up to which a simulation stays under each of the three error levels. For example, let's investigate more closely the coloured noise case for an altitude 300 km. If the given PSD has a noise level for higher frequencies of $10^{-12} \sqrt{\text{Hz}}$, a 0.1 mm geoid (black solid line) can be computed up to SH degree 124. Alternatively 1 mm, is reached at SH degree 176. It can be observed, that the different noise assumptions – white or coloured – primarily affect the lower degrees. This is clear, if one again refers to the image on the right side of Figure 1.

With these values one can derive requirements for the ranging sensor system (coloured noise case) for different altitudes. For altitudes higher than 400 km, the CGE for SH degrees 150, 200 and 250 will be higher than the required values. This means, that 10^{-14} is not sufficient for these altitudes. In the lower cases, the following noise levels would arise from the requirements in Table 3.

| Altitude [km] | required noise level | resulting CGE [mm] for SH degrees | | |
|---------------|----------------------|-----------------------------------|------|------|
| | | 150 | 200 | 250 |
| 300 | 3,E-13 | 0.10 | 0.95 | 10.3 |
| 350 | 5,E-14 | 0.04 | 0.66 | 10.3 |
| 400 | 1,E-14 | 0.02 | 0.55 | 12.3 |

Table 4: SST sensor requirements for three altitudes for a distance of 100 km (coloured noise case)

A summary of all requirements for different sensors, altitudes and distances can be seen in Chapter 5.

4.2 Accelerometer

Here the influence of the accelerometer sensor system shall be analyzed. One can see the same simulation approach as for the SST case. Different error levels are introduced as noise level for a white and a coloured noise case (see Figure 5). The model for the coloured noise case is

$$\delta\ddot{d}(f) = \begin{cases} a \cdot \left(\frac{0.001}{f}\right)^3, & f < 1 \text{ mHz} \\ a, & 1 \text{ mHz} \leq f \leq 100 \text{ mHz} \\ a \cdot \left(\frac{f}{0.1}\right)^2, & f > 100 \text{ mHz} \end{cases} \frac{\text{m}}{\text{s}^2 \sqrt{\text{Hz}}}, \quad a \in \{5 \cdot 10^{-10}; 4 \cdot 10^{-10}; 3 \cdot 10^{-10}; \dots; 5 \cdot 10^{-13}\}$$

The simulation results for d=100 km can be seen in the Figures 6, 7 and 8 (Appendix B contain the other distances).

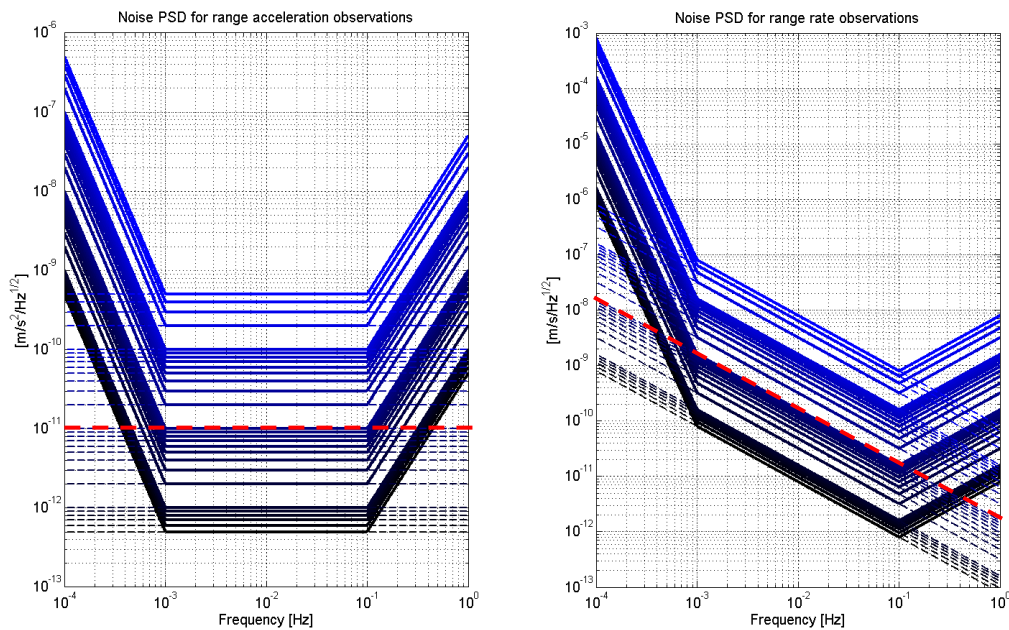


Figure 5: Noise PSDs in terms of range acceleration and range rate observations for the accelerometer sensor system (solid lines: coloured noise, dashed lines: white noise, red lines: Previous NGGM study limit)

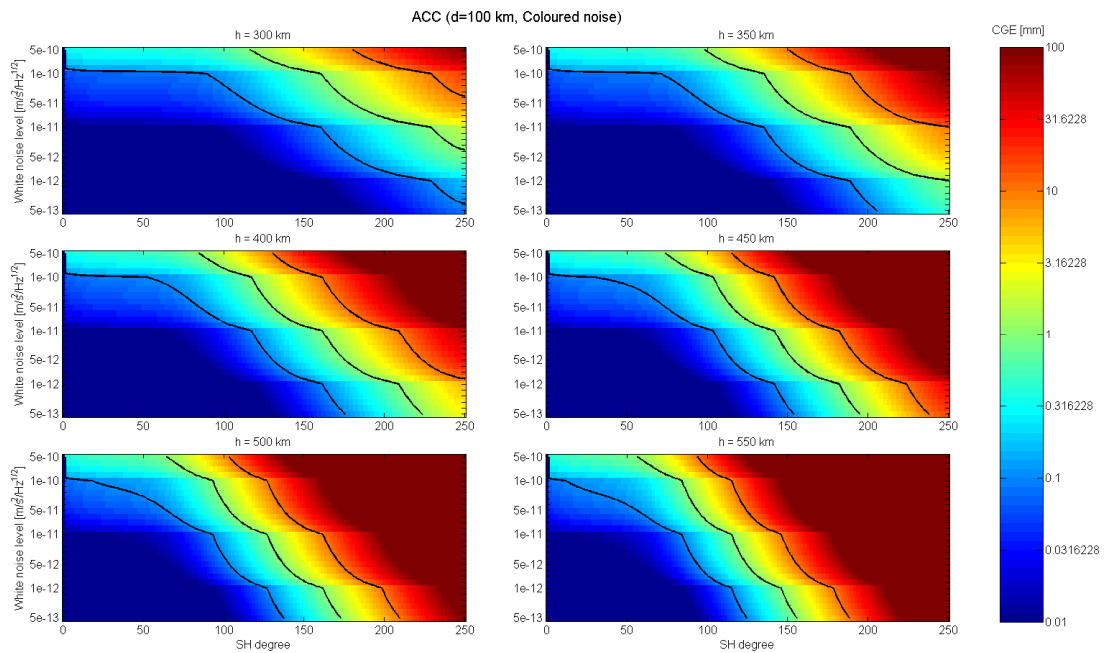


Figure 6: Cumulative Geoid Error for the accelerometer system for $d=100$ km, coloured noise case (the three black lines in each plot represent the CGE levels 0.1, 1 and 10 mm)

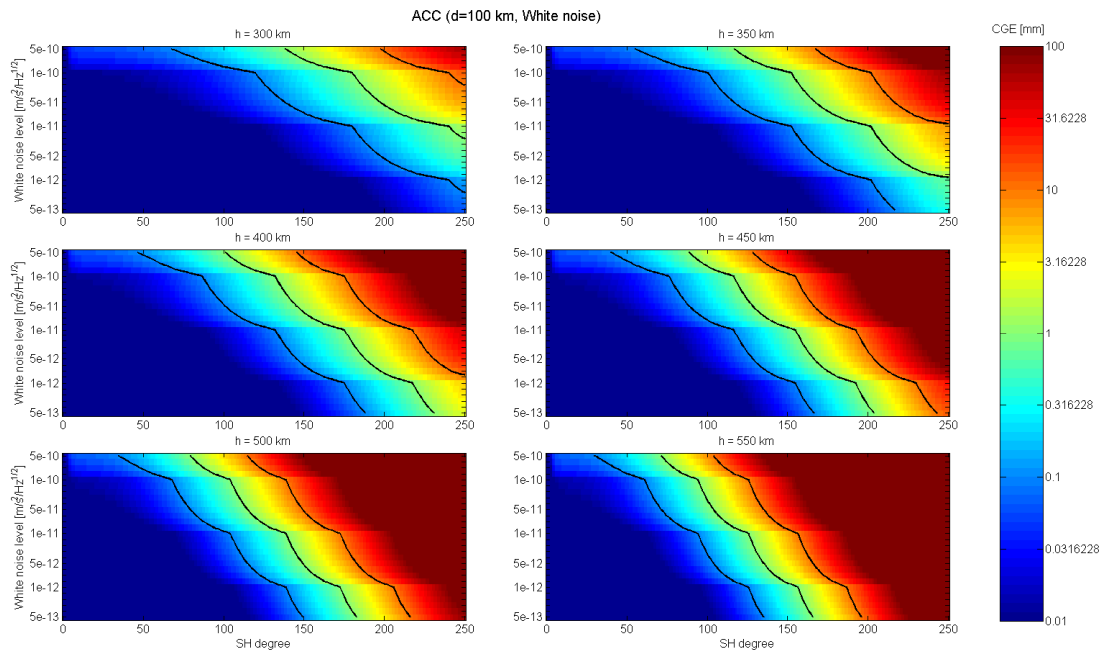


Figure 7: Cumulative Geoid Error for the accelerometer system for $d=100$ km, white noise case (the three black lines in each plot represent the CGE levels 0.1, 1 and 10 mm)

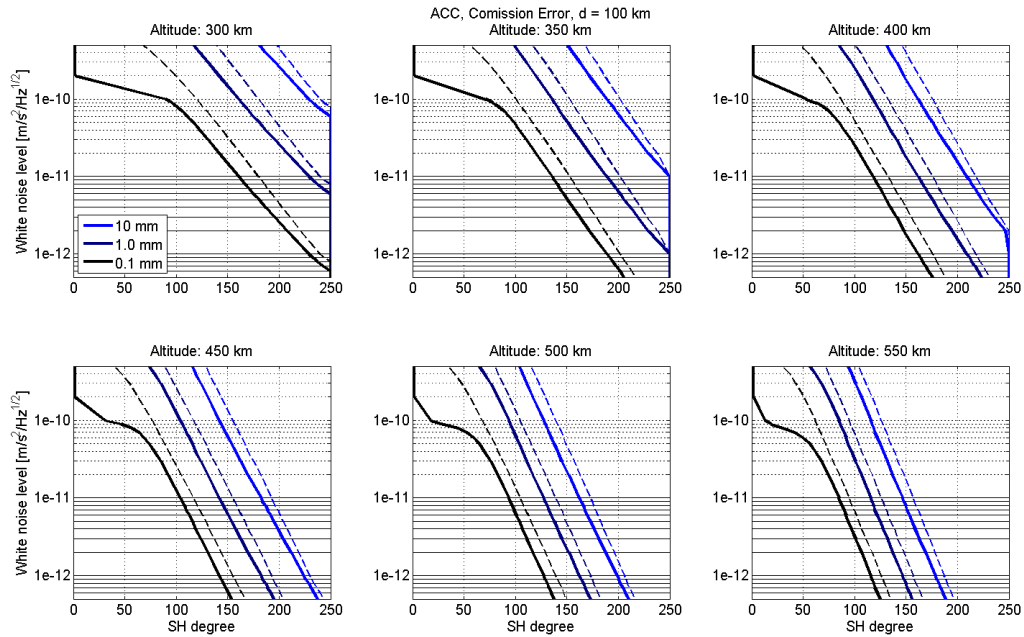


Figure 8: Requirement lines for the accelerometer for $d=100$ km (solid lines: coloured noise, dashed lines: white noise)

4.3 Alternative error scenario

One further error scenario is analyzed in this chapter. It contains noise PSDs for the satellite-to-satellite distance measurement and for the non-gravitational relative acceleration measurement. It holds for the mean distance between the satellites of 75 km (See 4).

Model of the satellite-to-satellite distance measurement error spectral density:

$$\delta\tilde{d}(f) = \begin{cases} 20 \cdot 10^{-9} & , f \geq 0.01 \text{ Hz} \\ 20 \cdot 10^{-9} \cdot \left(\frac{0.01}{f}\right) & , f < 0.01 \text{ Hz} \end{cases} \frac{\text{m}}{\sqrt{\text{Hz}}}$$

Model of the non-gravitational relative acceleration measurement error spectral density:

$$\delta\tilde{a}_d(f) = \begin{cases} 10^{-11} & , 0.001 \text{ Hz} \leq f \leq 0.01 \text{ Hz} \\ 10^{-11} \cdot \left(\frac{0.001}{f}\right)^2 & , f < 0.001 \text{ Hz} \\ 10^{-11} \cdot \left(\frac{f}{0.01}\right)^2 & , f > 0.01 \text{ Hz} \end{cases} \frac{\text{m}}{\text{s}^2 \sqrt{\text{Hz}}}$$

¹ In 4 there is 0.1 Hz as starting frequency for the upper part. But the figure in 4 shows 0.01 Hz. Here 0.01 Hz is chosen.

A graphical representation of this error scenario can be seen in Figure 9 in terms of range rate observations.

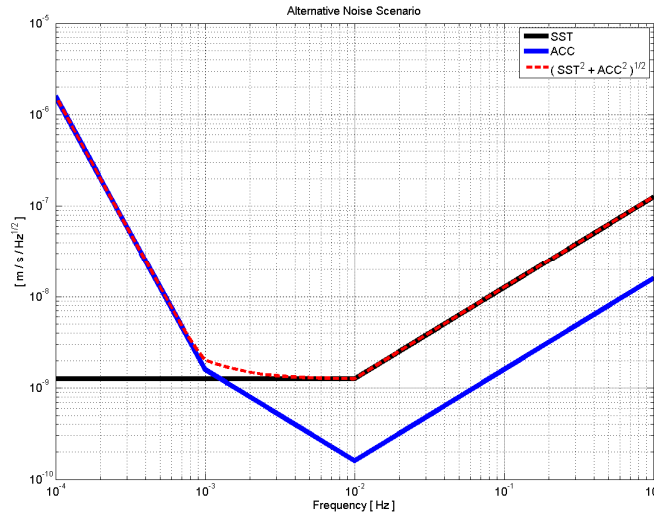


Figure 9: Alternative noise scenario for a mean distance of 75 km

The differences to the non-gravitational relative acceleration measurement error scenarios in 4.2 are the $\frac{1}{f^2}$ behaviour (instead of $\frac{1}{f^3}$) for the lower frequencies and the $\frac{1}{f^2}$ behaviour for frequencies above 10 mHz (instead of 100 mHz). The second difference will not lead to very different CGEs for the combined case (SST and ACC) because the high frequencies are dominated by the SST noise (See also Figure 13). The simulation results in terms of CGEs are presented in the same way as Figure 6 for six different mission altitudes.

Therefore several noise levels are analyzed. Different levels are computed by taking the alternative noise models from above and decrease step by step the first factor. This is represented by the number k (k=0 stands for the two numbers from above: $20 \cdot 10^{-9}$ for the SST and 10^{-11} for the ACC sensor). All chosen levels are listed in Table 5.

| K | SST | ACC | k | SST | ACC |
|----|--------|--------|----|--------|--------|
| 0 | 2,E-08 | 1,E-11 | 11 | 9,E-10 | 8,E-13 |
| 1 | 1,E-08 | 9,E-12 | 12 | 8,E-10 | 7,E-13 |
| 2 | 9,E-09 | 8,E-12 | 13 | 7,E-10 | 6,E-13 |
| 3 | 8,E-09 | 7,E-12 | 14 | 6,E-10 | 5,E-13 |
| 4 | 7,E-09 | 6,E-12 | 15 | 5,E-10 | 4,E-13 |
| 5 | 6,E-09 | 5,E-12 | 16 | 4,E-10 | 3,E-13 |
| 6 | 5,E-09 | 4,E-12 | 17 | 3,E-10 | 2,E-13 |
| 7 | 4,E-09 | 3,E-12 | 18 | 2,E-10 | 1,E-13 |
| 8 | 3,E-09 | 2,E-12 | 19 | 1,E-10 | 9,E-14 |
| 9 | 2,E-09 | 1,E-12 | 20 | 9,E-11 | 8,E-14 |
| 10 | 1,E-09 | 9,E-13 | | | |

Table 5: Different error levels for the alternative noise scenario

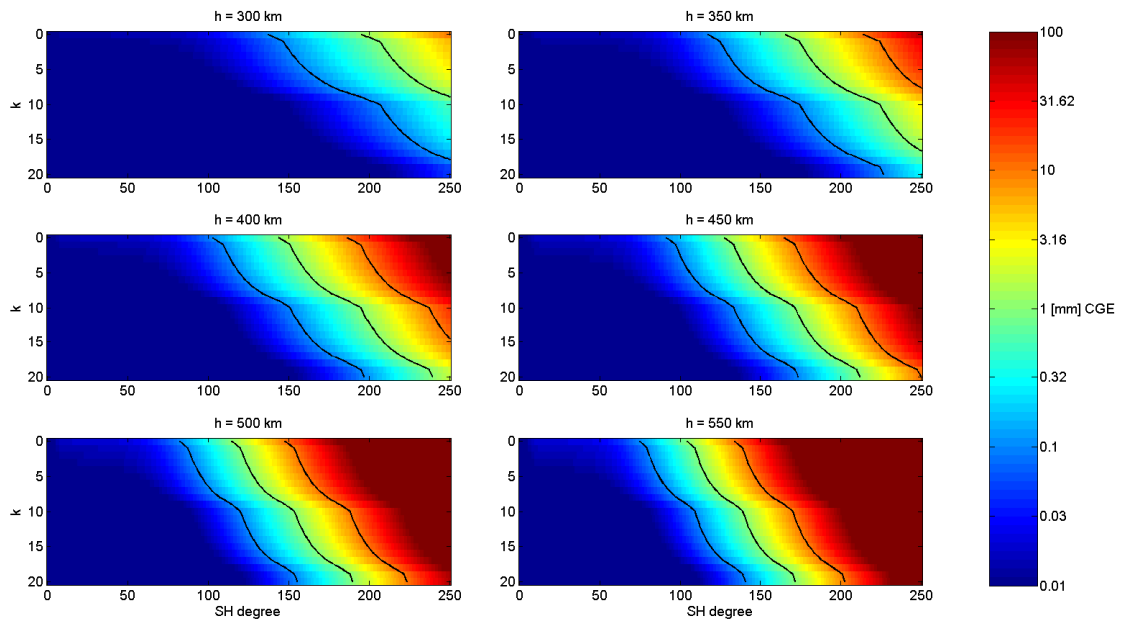


Figure 10: Cumulative Geoid Error for $\sqrt{SST^2 + ACC^2}$
for $d=75$ km, alternative error scenario.

The three black lines in each plot represent the CGE levels 0.1, 1 and 10 mm.
The y-axis k stands for different error levels (See Table 5)

These results then lead to requirements for k to reach the science requirements of Table 3. The required numbers k can be seen in Table 6 with their noise levels for the two types of sensors and the resulting CGEs.

| Altitude [km] | k | SST | ACC | CGE [mm] | | |
|------------------|----|--------|--------|----------|------|-------|
| | | | | 150 | 200 | 250 |
| 300 | 3 | 8,E-09 | 7,E-12 | 0.09 | 0.62 | 4.31 |
| 350 | 8 | 3,E-09 | 2,E-12 | 0.09 | 0.86 | 9.09 |
| 400 | 15 | 5,E-10 | 4,E-13 | 0.05 | 0.64 | 9.32 |
| 450 | 20 | 9,E-11 | 8,E-14 | 0.02 | 0.49 | 10.15 |

Table 6: required noise levels for the alternative error scenario

4.4 GNSS

Observations of orbit perturbations are not as important as range or accelerometer observations. In general their information is needed to locate the range observations. In a combined gravity field solution this affects only the very low SH degrees. Nevertheless it is important to define sufficient requirements for this observation type as well. In general it can be said that the noise of GNSS observations, i.e. the derived satellite positions should be on a centimetre level. In terms of noise PSDs a figure like the left image of Figure 11 can be expected. Typical noise PSDs for GNSS observations have a white noise behaviour with a maximum around the orbit frequency.

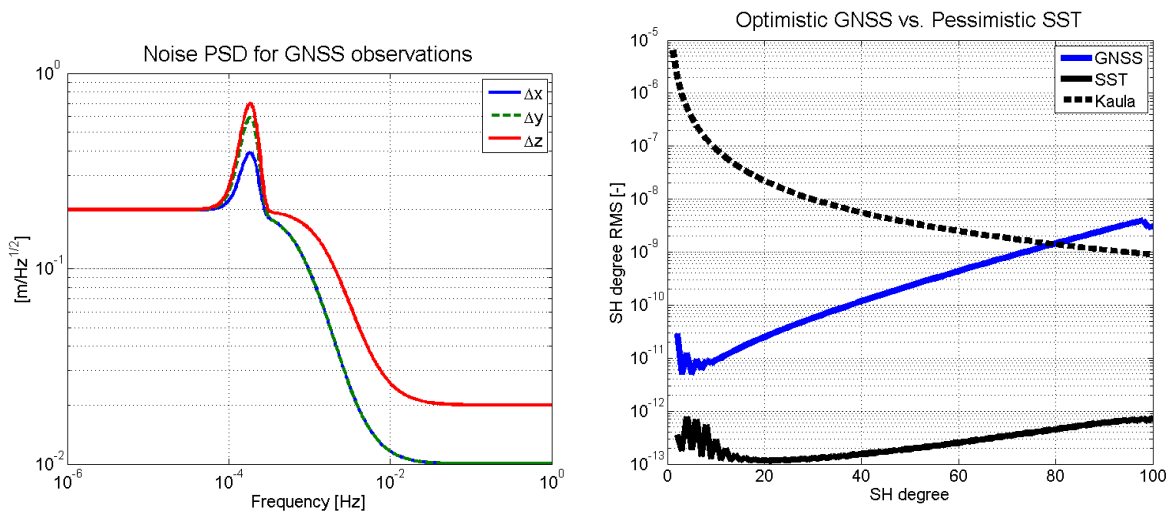


*Figure 11, left: Typical noise PSD for LEO positions derived by GNSS (x: along-track, y: cross-track, z: radial)
right: SH degree RMS comparison of an optimistic GNSS simulation and a pessimistic SST simulation (d=100 km, h=300 km)*

A sensitivity analysis shows that SST gravity field analysis don't get much profit from GNSS observations. As mentioned before they are mainly used for locating the SST observations in space. The right image of Figure 11 shows SH degree RMS values for the most pessimistic SST performance of Figure 1 compared with an optimistic GNSS performance. This is a white noise behaviour on a level of $1 \frac{cm}{\sqrt{Hz}}$. It can be observed that the SH degree RMS of the SST simulation stays at least one order of magnitude beyond the GNSS simulation.

4.5 Gradiometry

4.5.1 Sensitivity

The sensitivity of satellite gravity gradiometry (SGG) for the lower SH degrees is very low. Therefore GNSS or SST observations are needed in addition. Without this combination the cumulative errors would be dominated by very large errors in the lower SH degrees. For that purpose again a sensitivity analysis can be seen in the right image of Figure 12. It shows four pessimistic SST simulations compared with SGG simulations in terms of SH degree RMS (only zz-component of the gradient tensor is applied as observation). A full gradiometer could improve that zz-only solution by a factor of 1.5 in terms of SH degree RMS. For gradiometry, noise PSDs of different quality levels are assumed, which can be seen in the left image of Figure 12.

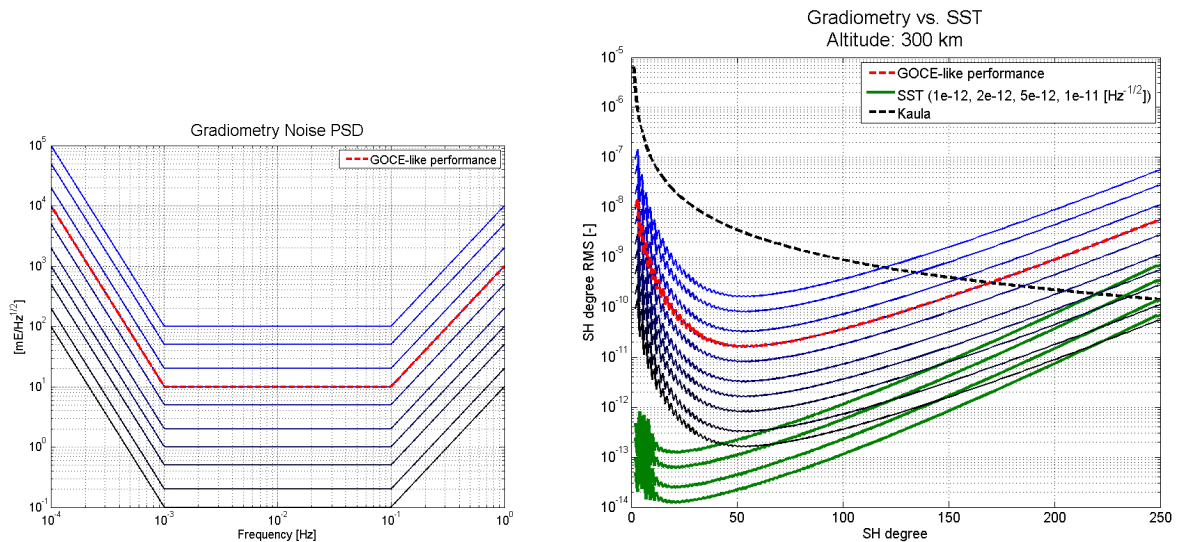


Figure 12, left: Typical noise PSDs for Gradiometry observations
right: SH degree RMS comparison of Gradiometry simulations (blue and black curves)
and SST simulations ($d=100$ km, $h=300$ km), the SST performances shown here have
white noise levels of $n \cdot 10^{-7} \left[\frac{m}{\sqrt{Hz}} \right]$ with $n \in \{1, 2, 5, 10\}$

Let's investigate more closely the right image of Figure 12. There the SH degrees can be detected, where gradiometry observations could improve a SST gravity field (at least in that example for an altitude of 300 km and a satellite separation of 100 km). The best gradiometry performance in Figure 12 represents approximately a 100 times better GOCE performance. The best SST performance in that plot has a white noise level of $10^{-7} \left[\frac{m}{\sqrt{Hz}} \right]$, which is two times worse than the previous NGGM study limit. If one compares these two SH degree RMS curves, it can be observed, that only for the highest SH degrees over approx. 220 an improvement from gradiometry can be expected.

4.5.2 Redundancy and CGE

The previous section shows comparisons in terms of SH degree RMS of separate simulations for SST or SGG. Now a combination of both sensors on one satellite shall be compared with a SST only simulation.

The SGG noise scenario shown in Figure 12 left has the same characteristics as the initial acceleration error scenarios (see Figure 5). For the following analyses an error scenario is chosen, which is adopted from the alternative scenario for the non-gravitational relative acceleration measurements (see chapter 4.3). The other simulation parameters holding for that example are an altitude of 300 km and a mean distance between the satellites of 75 km. We know from the previous section, that we have to go down with the white noise level to 0.1 mE to get a better sensitivity for the very high degrees in terms of RMS per degree. This noise level is chosen for the following simulations. Therefore the model for the SGG observations can be described as

$$\delta\tilde{g}(f) = \begin{cases} 10^{-1} \cdot \left(\frac{0.001}{f}\right)^2, & f < 0.001\text{Hz} \\ 10^{-1}, & 0.001\text{Hz} \leq f \leq 0.01\text{Hz} \\ 10^{-1} \cdot \left(\frac{f}{0.01}\right)^2, & f > 0.01\text{Hz} \end{cases} \frac{\text{mE}}{\sqrt{\text{Hz}}}$$

For the range rate observations the alternative error scenario described in 4.3 holds (Figure 9, red dashed line). This range rate observations lead to a SH error characteristic as in the upper image of Figure 13. It shows the typical error behaviour for that type of observations: very high sensitivity for the low degrees and low orders, worse sensitivity for high orders (sectorial coefficients).

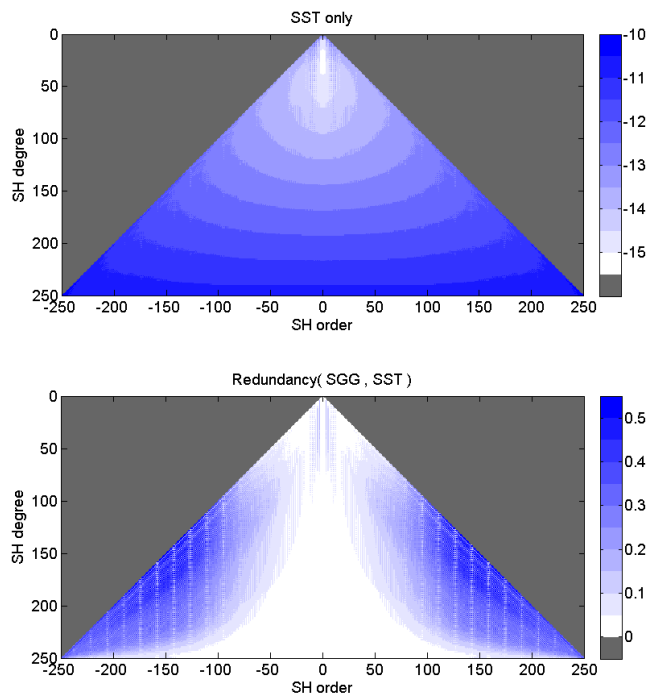


Figure 13, top: SH error spectrum of an SST only solution (alternative error scenario, altitude 300 km, distance 75 km, log₁₀ scaling)
down: Redundancy of SST-SGG combination compared to SST-only

The lower image of Figure 13 shows the redundancy of the combination of SST and SGG compared to SST only in terms of variances. For every SH order and degree the redundancy is $r = 1 - \frac{\sigma_{SST+SGG}^2}{\sigma_{SST}^2}$. So a redundancy of 0.1 means a ten percentage reduction

of the SST only variance by combining it with SGG.

What this means in terms of CGE can be seen in Figure 14. On the left side the cumulative errors slightly above the requirements (0.1 mm for SH degree L=150, 1 mm for L=200 and 10 mm for L=250) for the combination and SST only can be seen. The difference is in the order of one magnitude less. On the right side the improvements are plotted, which have their maximum around L=150 at about 22 %.

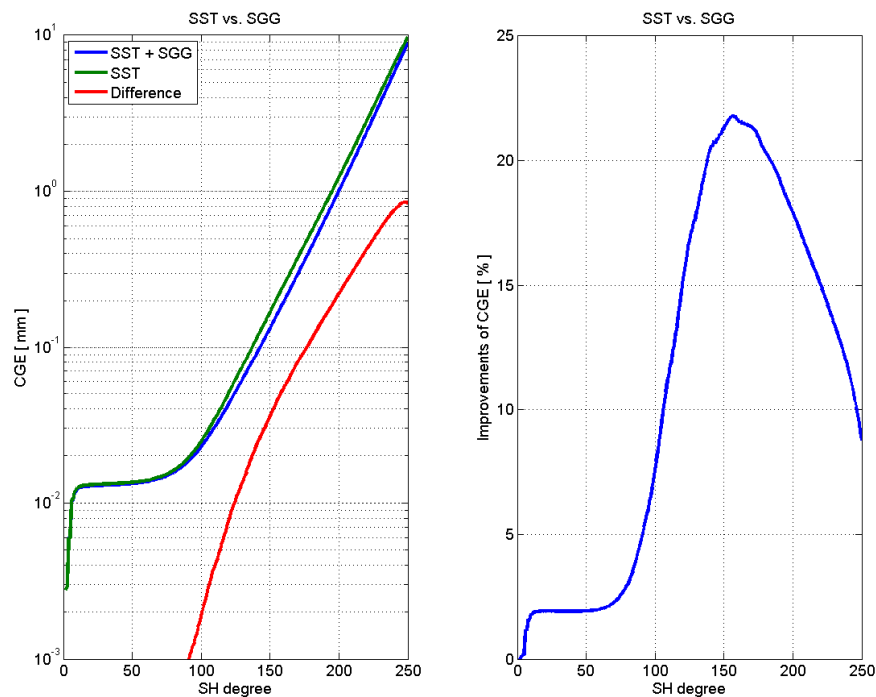


Figure 14, left: CGEs of SST-SGG combination compared to SST only
right: improvements of SST only CGEs by combination with SGG

So to sum up the gradiometry part, it can be said, that a low-low SST mission wont get much benefit from additional SGG observations in terms of geoid errors. What can be expected is nevertheless a more isotrope error structure of the combined solution. This is because of the higher sensitivity in the combined case of the sectorials (see Figure 13).

5. Summary

In this Chapter a summary of all the simulations done for this document shall be presented. The main goal is the definition of requirements for each sensor. Therefore here the requirements for the SST and the accelerometer sensors are placed. Table 7 shows for each here simulated altitudes and satellite distances and for the two sensor types a value of maximum noise level. This noise level represents for the SST sensor the relative noise level for frequencies above 10mHz in $\left[\frac{1}{\sqrt{\text{Hz}}}\right]$ (See Figure 1). For the accelerometer it is the noise level for $1\text{mHz} < f < 100\text{mHz}$ in $\left[\frac{\text{m}^2}{\sqrt{\text{Hz}}}\right]$ (See Figure 5). These requirements directly come from the CGE requirement Table 3. To reach the values of Table 3, the noise level of the sensor mustn't be larger than the values in Table 7 in each of the different profiles for altitude and distance.

| | | Satellite Separation [km] | | | | | | | | |
|-----|---------------|---------------------------|---------|---------|---------|---------|---------|---------|---------|---------|
| | | 50 | | 100 | | 200 | | 300 | | |
| | | wn | cn | wn | cn | wn | cn | wn | cn | |
| SST | Altitude [km] | 300 | 5,E-13 | 4,E-13 | 4,E-13 | 3,E-13 | 4,E-14 | 4,E-14 | 3,E-14 | 3,E-14 |
| | | 350 | 8,E-14 | 7,E-14 | 6,E-14 | 5,E-14 | <1,E-14 | <1,E-14 | <1,E-14 | <1,E-14 |
| | | 400 | 2,E-14 | 2,E-14 | <1,E-14 | <1,E-14 | <1,E-14 | <1,E-14 | <1,E-14 | <1,E-14 |
| | | 450 | <1,E-14 |
| | | 500 | <1,E-14 |
| | | 550 | <1,E-14 |
| | | 600 | <1,E-14 |
| ACC | Altitude [km] | 300 | 2,E-11 | 8,E-12 | 4,E-11 | 2,E-11 | 7,E-11 | 3,E-11 | 9,E-11 | 5,E-11 |
| | | 350 | 6,E-12 | 3,E-12 | 2,E-11 | 6,E-12 | 3,E-11 | 2,E-11 | 3,E-11 | 2,E-11 |
| | | 400 | 2,E-12 | 8,E-13 | 3,E-12 | 2,E-12 | 5,E-12 | 3,E-12 | 6,E-12 | 5,E-12 |
| | | 450 | <5,E-13 | <5,E-13 | <5,E-13 | <5,E-13 | 8,E-13 | 6,E-13 | 1,E-12 | 9,E-13 |
| | | 500 | <5,E-13 |
| | | 550 | <5,E-13 |
| | | 600 | <5,E-13 |

Table 7: Requirements for the SST sensor and the accelerometer to meet the required CGE values of Table 3 (wn: white noise, cn: coloured noise). Every mission profile belonging to a grey box will not meet the requirements with the minimum noise levels. The different colours should mark different levels (e.g. SST green: $\{1; 2; 3; 4; 5\} \cdot 10^{-13}$, yellow: $\{6; 7; 8; 9\} \cdot 10^{-14}$ and orange: $\{1; 2; 3; 4; 5\} \cdot 10^{-14}$)

$$\{6; 7; 8; 9\} \cdot 10^{-14} \text{ and orange: } \{1; 2; 3; 4; 5\} \cdot 10^{-14}$$

The next question is which errors will arise from both sensors together SST and accelerometer. This could be simulated in the same way using the square root of the quadratic sum of both noise PSDs. Figure 15 shows this combined case for the distance of 100 km and an altitude of 300 km.

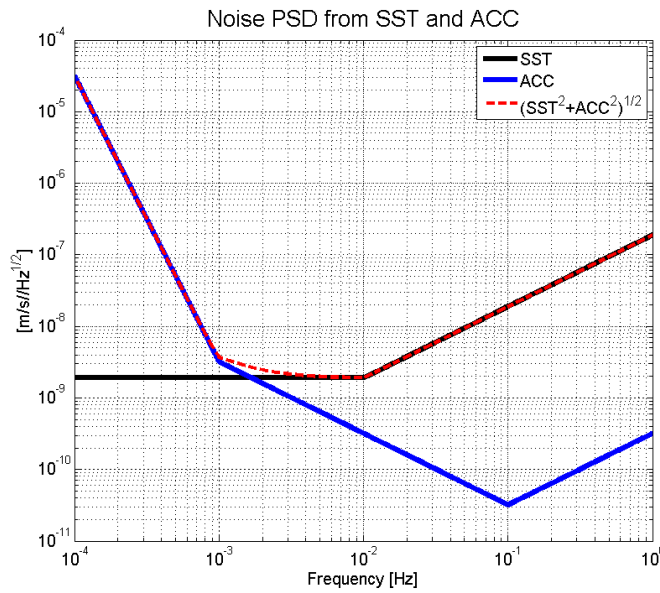


Figure 15: Noise PSD in terms of range rates from SST sensor ($d=100$ km, white noise level: $3 \cdot 10^{-13} \text{ } \frac{1}{\sqrt{\text{Hz}}}$) and accelerometer (white noise level: $2 \cdot 10^{-11} \text{ } \frac{\text{m/s}^2}{\sqrt{\text{Hz}}}$)

Applying the red dashed noise PSD curve to the simulation one gets the following results for CGE (See Figure 16). In addition the results of one and two steps better behaviour are shown. These are $2 \cdot 10^{-13} \text{ } \frac{1}{\sqrt{\text{Hz}}}$ and $1 \cdot 10^{-13} \text{ } \frac{1}{\sqrt{\text{Hz}}}$ for the white noise level of the SST sensor and $1 \cdot 10^{-11} \text{ } \frac{\text{m/s}^2}{\sqrt{\text{Hz}}}$ and $9 \cdot 10^{-12} \text{ } \frac{\text{m/s}^2}{\sqrt{\text{Hz}}}$ for the white noise level of the accelerometer.

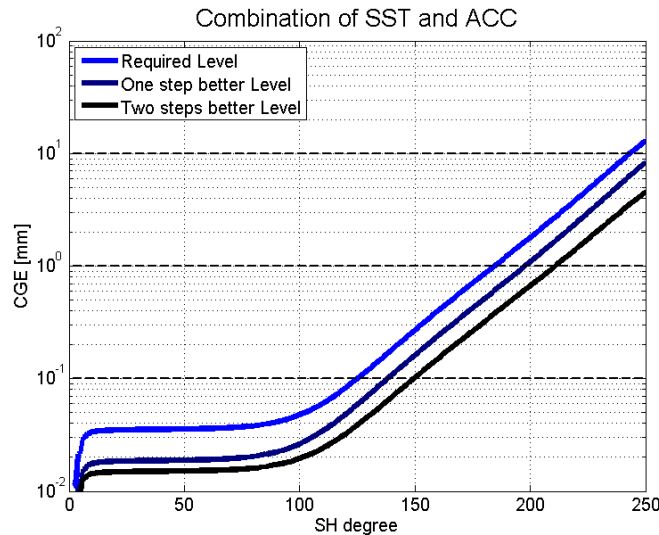


Figure 16: CGE for a combination of SST and ACC noise

From Figure 16 it can be seen, that in a combined case of SST sensor and accelerometer noise the required level of Table 7 for each of the sensors is slightly not sufficient to reach the required CGE values of Table 3. This is clear, if one looks at Figure 15. In that case of an altitude of 300 km and a distance of 100 km it can be observed, that the requirements are met if we apply noise levels of two steps better for each sensor.

5.1 Alternative error scenario

In the alternative error scenario (see chapter 4.3) the noise levels are slightly different and can be computed with the values in Table 6 and the Formulas in 4.3. For one example the model shall be presented here in an analytical and a graphical way. This is again the altitude 300 km and the distance 75 km. From Table 6 it follows, that k must be 3 and therefore the white noise levels of the SST part is 8E-9 and for the ACC part 7E-12. So it holds

$$\delta\tilde{d}(f) = \begin{cases} 8 \cdot 10^{-9} & , f \geq 0.01\text{Hz} \\ 8 \cdot 10^{-9} \cdot \left(\frac{0.01}{f}\right) & , f < 0.01\text{Hz} \end{cases} \frac{\text{m}}{\sqrt{\text{Hz}}}$$

and

$$\delta\tilde{d}_D(f) = \begin{cases} 7 \cdot 10^{-12} & , 0.001\text{Hz} \leq f \leq 0.01\text{Hz} \\ 7 \cdot 10^{-12} \cdot \left(\frac{0.001}{f}\right)^2 & , f < 0.001\text{Hz} \\ 7 \cdot 10^{-12} \cdot \left(\frac{f}{0.01}\right)^2 & , f > 0.01\text{Hz} \end{cases} \frac{\text{m}}{\text{s}^2 \sqrt{\text{Hz}}}$$

Figure 15 shows the required noise spectrum in terms of range rates (left) and range accelerations (right).

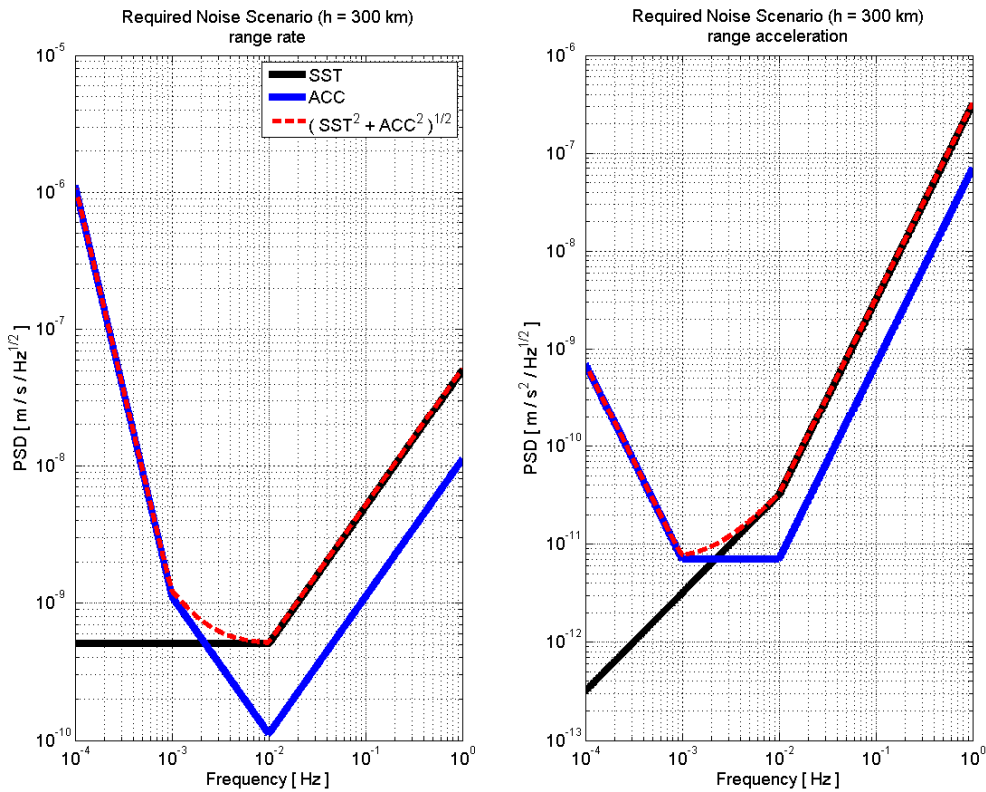


Figure 17: Required error scenario for SST and ACC for an altitude of 300 km (left in terms of range rates, right in terms of range accelerations)

6. Appendix

Appendix A: Error propagation for linear trend estimation

Preliminary Estimation:

There is a regular sampled time series of observations ($T=n$ [years], sampling: Δt [years]). Each observation is independent from the others and equal accurate (standard deviation: σ [mm]). The signal trend should be measured with an accuracy of σ_t [mm/year].

Question: Which value is sufficient for σ ?

The observation equation is the linear function $\hat{y} = \hat{a}t + \hat{b}$. The design matrix A and the weight matrix P of the least squares adjustment then are

$$A = \begin{pmatrix} \frac{\partial \hat{y}}{\partial \hat{a}} & \frac{\partial \hat{y}}{\partial \hat{b}} \end{pmatrix} = \begin{pmatrix} t_0 & 1 \\ t_0 + \Delta t & 1 \\ \vdots & \vdots \\ t_0 + T & 1 \end{pmatrix}, \quad P = \text{diag}(\sigma^{-2} \quad \dots \quad \sigma^{-2}).$$

For the normal equation matrix N it holds

$$N = (A^T P A) = \frac{1}{\sigma^2} \begin{pmatrix} \sum t^2 & \sum t \\ \sum t & n+1 \end{pmatrix} \text{ with } t = (t_0 \quad t_0 + \Delta t \quad \dots \quad t_0 + T) \text{ and } n = T/\Delta t.$$

The accuracy of the trend is the first element of the inverse of N . It is

$$\sigma_t = \sqrt{\frac{12\sigma^2}{\Delta t^2 (n-1)n(n+1)}}, \text{ so for } \sigma \text{ it follows:}$$

$$\sigma = \sigma_t \sqrt{\frac{T^3/\Delta t - \Delta t \cdot T}{12}} \approx \sigma_t \cdot T^{3/2}.$$

The last approximation holds for monthly measurements. In the case of the nominal mission profile it is an 11 years time series with monthly observations. The secular signal magnitude of signal 1 in Table 1 is 0.01 mm/year. With this approach one get a maximum standard deviation for one single observation of 0.36 mm. Therefore the value in Table 2 of 0.1 mm is obviously sufficient. The same holds for signal 2 in Table 1.

Appendix B: Simulation results

SST sensor:
Distance: 50 km

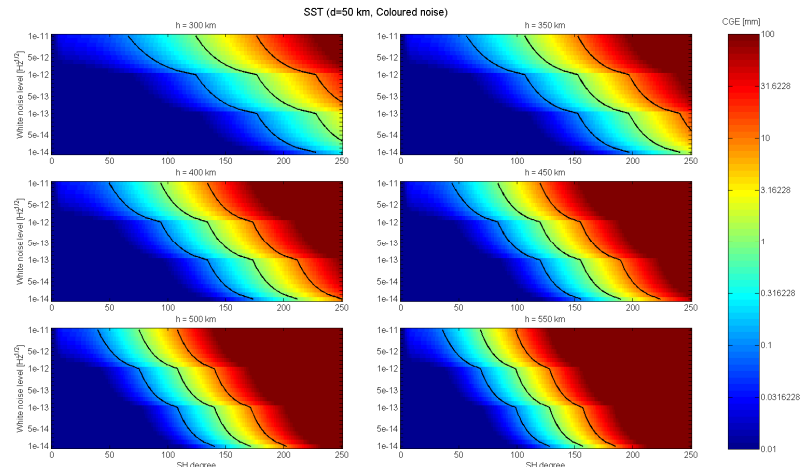


Figure B1: CGE for SST sensor, $d=50$ km, coloured noise case

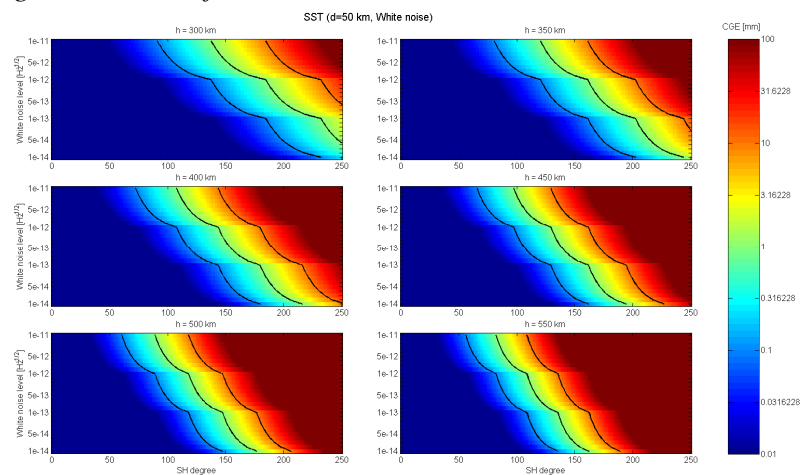


Figure B2: CGE for SST sensor, $d=50$ km, white noise case

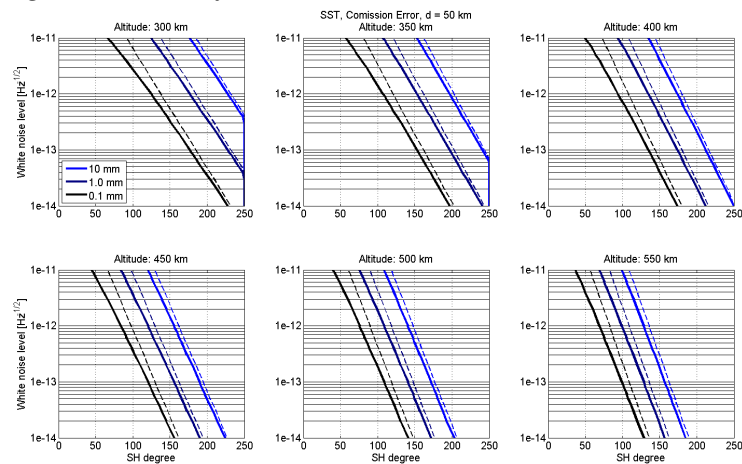


Figure B3: Requirement lines for SST sensor, $d=50$ km (solid lines: coloured noise, dashed lines: white noise)

SST sensor:
Distance: 200 km

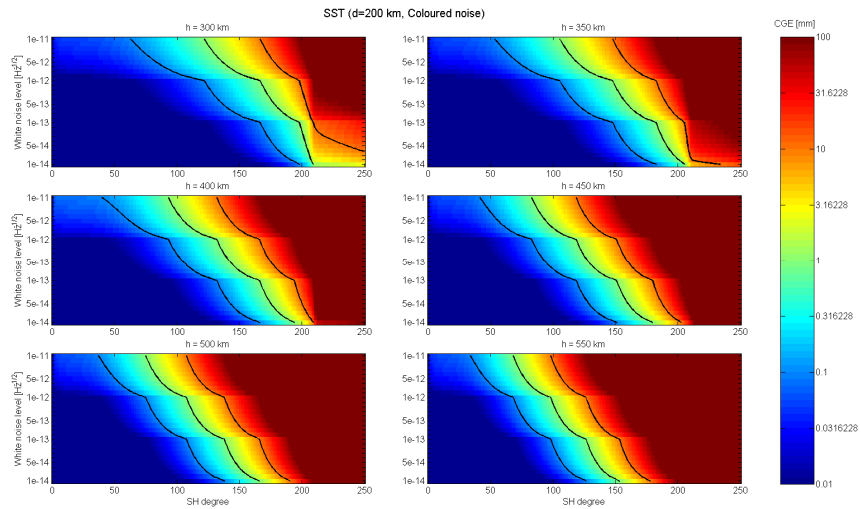


Figure B4: CGE for SST sensor, $d=200$ km, coloured noise case

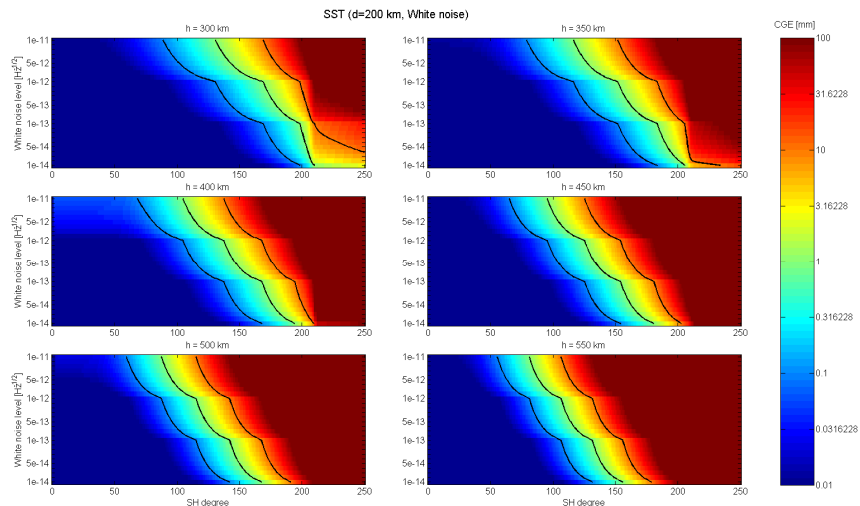


Figure B5: CGE for SST sensor, $d=200$ km, white noise case

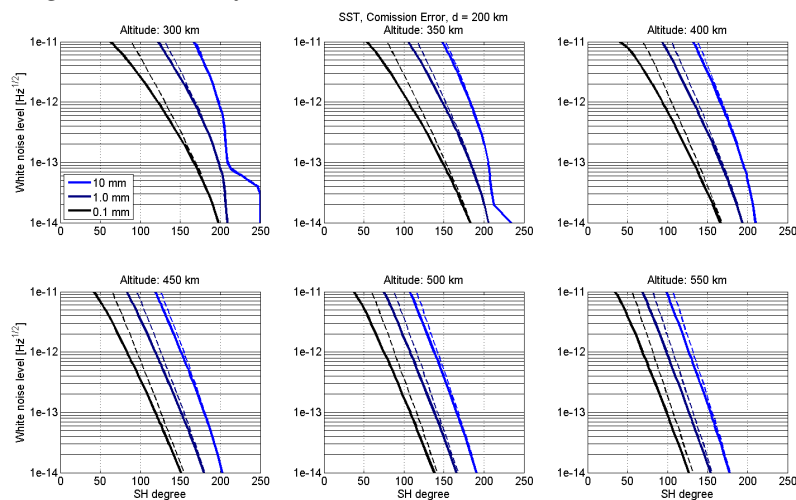


Figure B6: Requirement lines for SST sensor, $d=200$ km (solid lines: coloured noise, dashed lines: white noise)

SST sensor:
Distance: 300 km

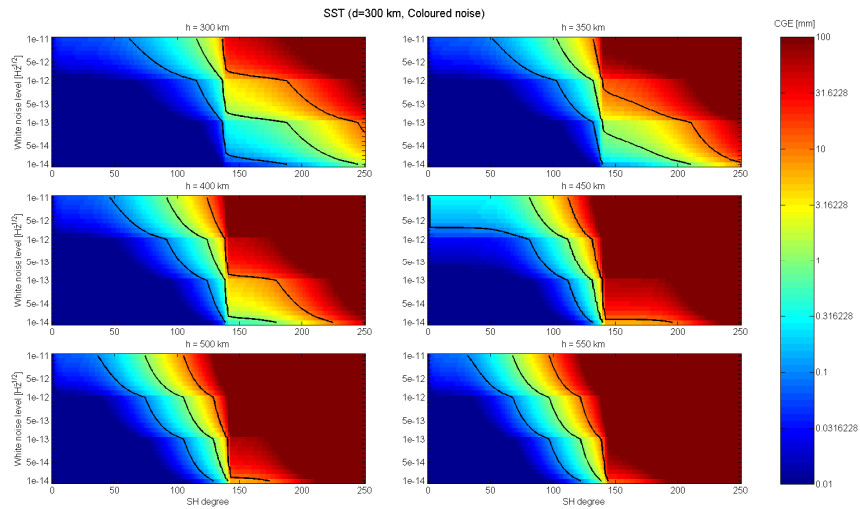


Figure B7: CGE for SST sensor, d=300 km, coloured noise case

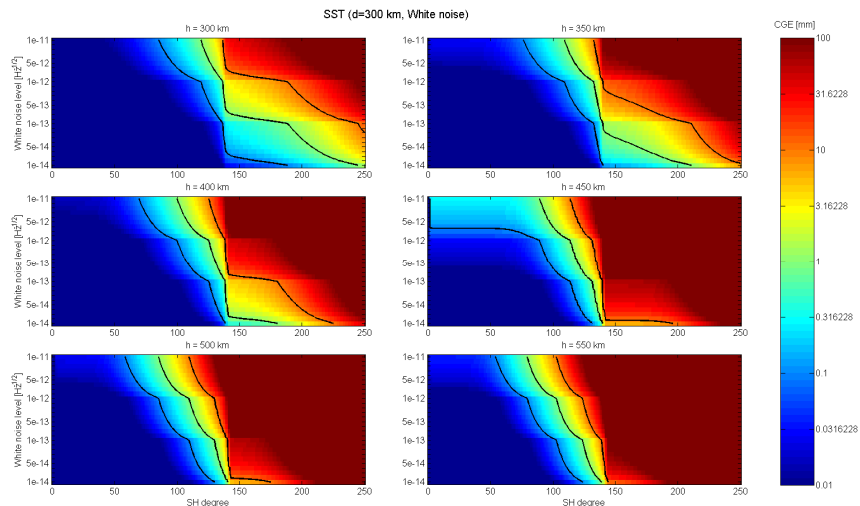


Figure B8: CGE for SST sensor, d=300 km, white noise case

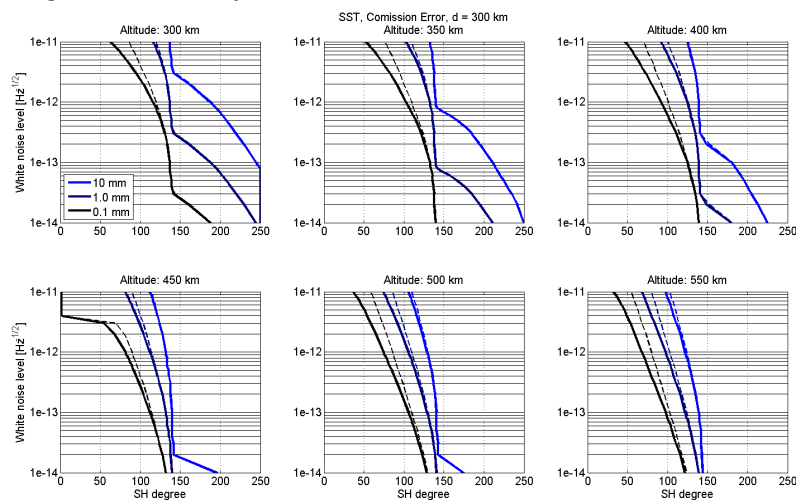
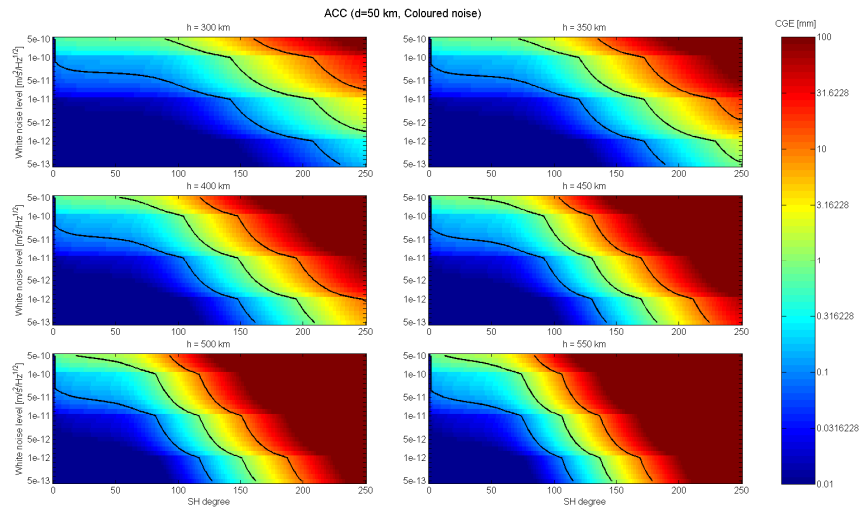


Figure B9: Requirement lines for SST sensor, d=300 km (solid lines: coloured noise, dashed lines: white noise)

Accelerometer:
Distance: 50 km



B10: CGE for Accelerometer, d=50 km, coloured noise case

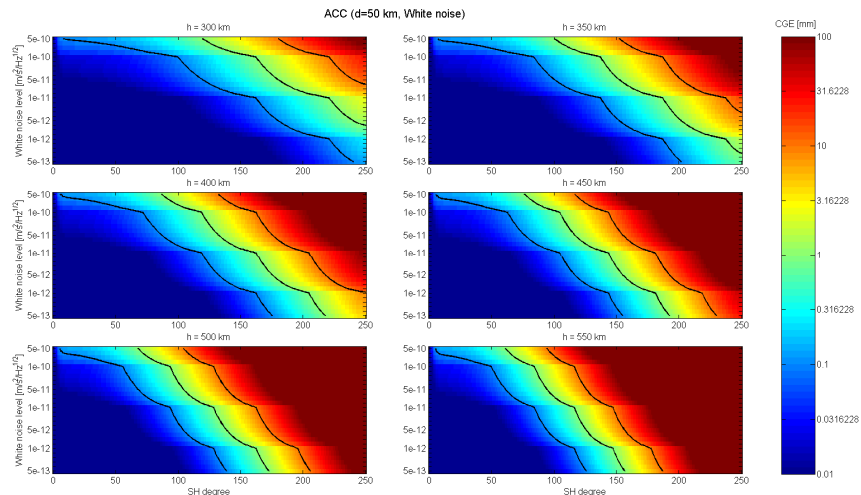


Figure B11: CGE for Accelerometer, d=50 km, white noise case

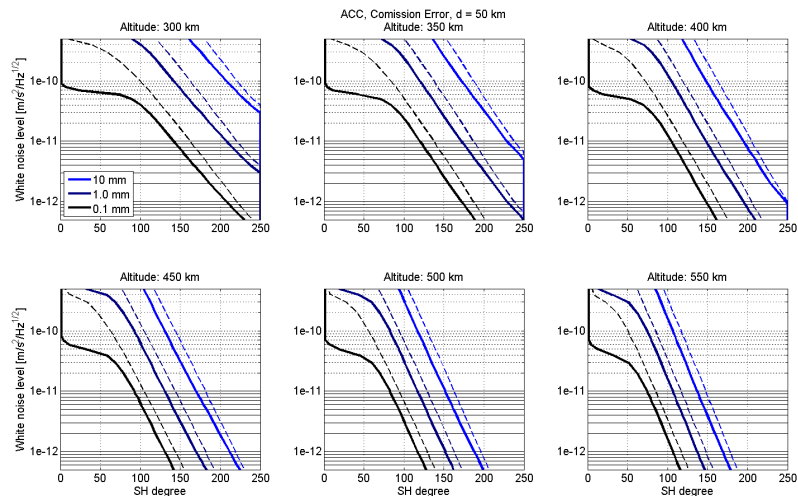
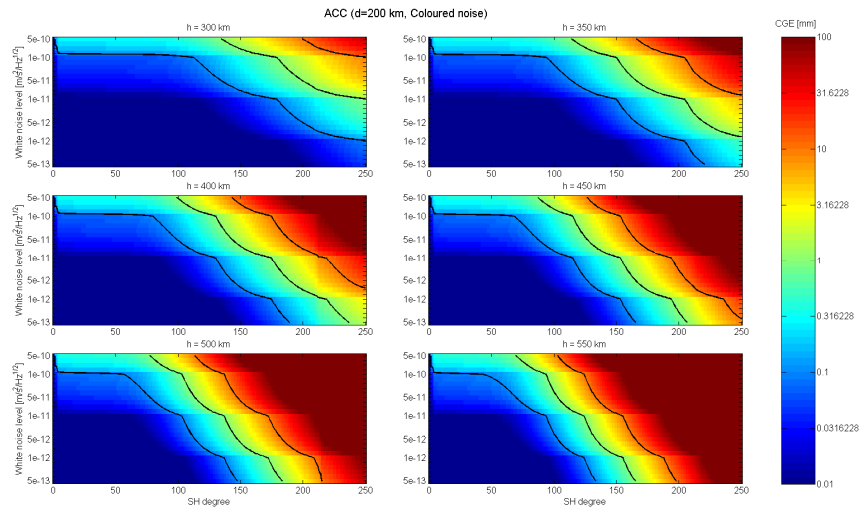


Figure B12: Requirement lines for Accelerometer, d=50 km (solid lines: coloured noise, dashed lines: white noise)

Accelerometer:
Distance: 200 km



B13: CGE for Accelerometer, d=200 km, coloured noise case

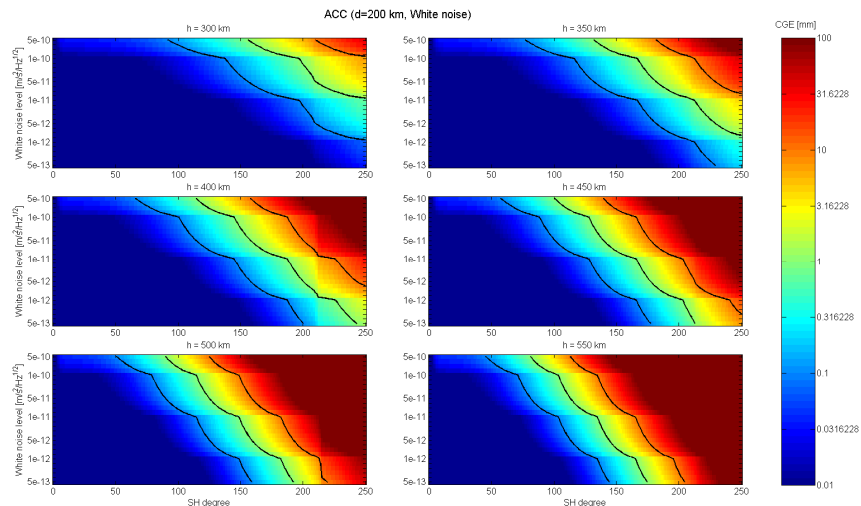


Figure B14: CGE for Accelerometer, d=200 km, white noise case

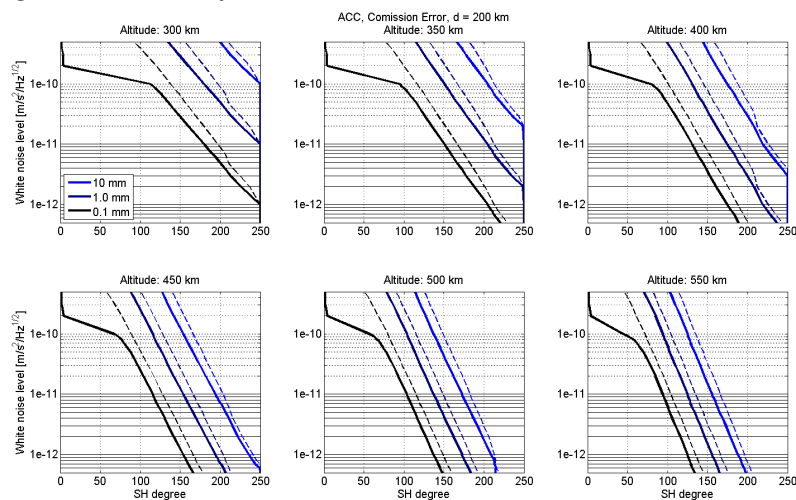
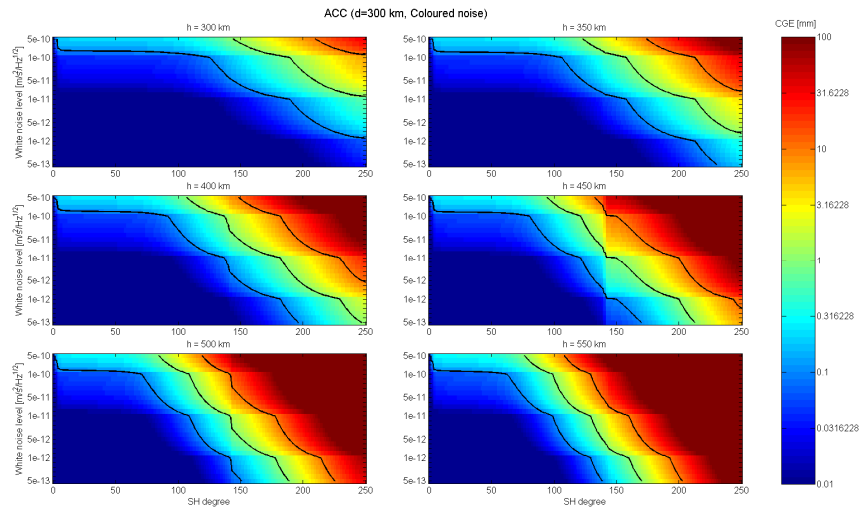


Figure B15: Requirement lines for Accelerometer, d=200 km (solid lines: coloured noise, dashed lines: white noise)

Accelerometer:
Distance: 300 km



B16: CGE for Accelerometer, d=300 km, coloured noise case

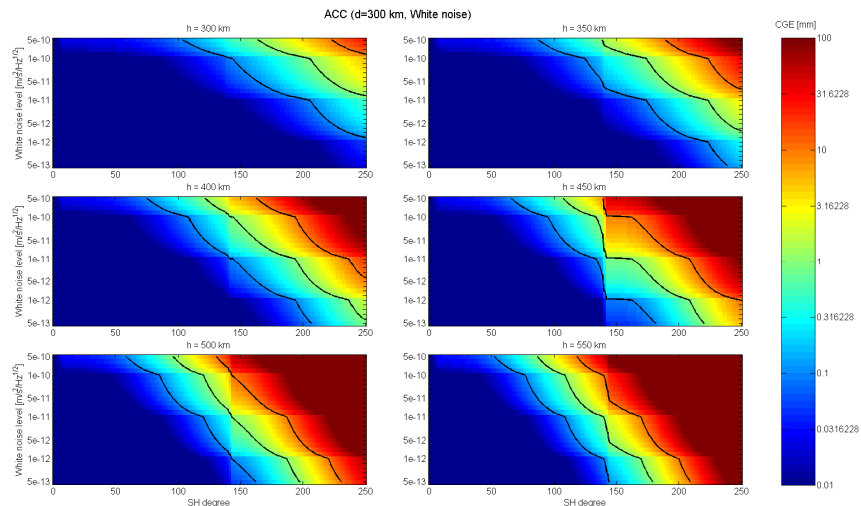


Figure B17: CGE for Accelerometer, d=300 km, white noise case

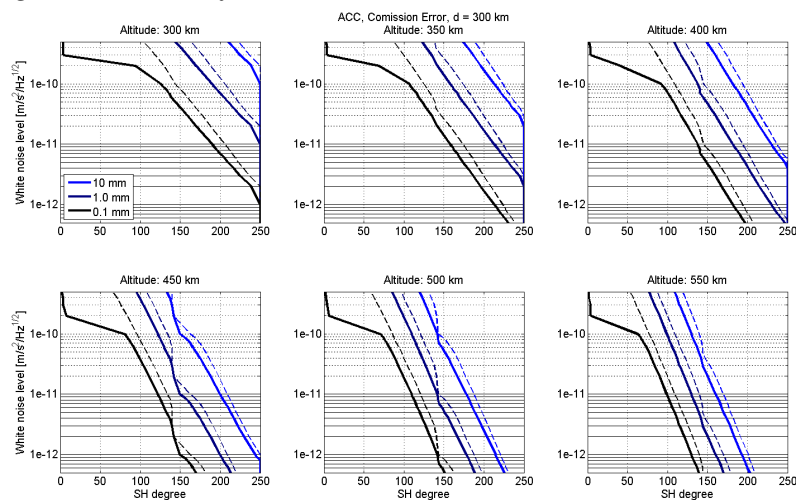


Figure B18: Requirement lines for Accelerometer, d=300 km (solid lines: coloured noise, dashed lines: white noise)

7. References

1. WP1100 Report DRAFT, Doc. No.: NGGM_SCI_1, task_1_v3.pdf (Issue: 1, Revision: 1, Date: 08-February, 2010)
2. WP1100: Requirements Analysis Progress Report, SD-MI-AI-1069 Annex1 NGGM_RRM_Ulux.pdf
3. SD-MI-AI-1069 Annex 2 NGGM_RRM_TASI.ppt (Requirements Review Meeting)
4. Reference error models for SST and ACC
TAS-I-Reference measurement noise for 75 km.doc